An Effective Dynamic Coarse Model for Optimization Design of LTCC RF Circuits With Aggressive Space Mapping

Ke-Li Wu, *Senior Member, IEEE*, Yong-Jiu Zhao, Jie Wang, and Michael K. K. Cheng, *Member, IEEE*

***Abstract*—A new concept called the dynamic coarse model is proposed and is applied to the optimization design of low-temperature co-fired ceramic (LTCC) multilayer RF circuits with the aggressive space mapping (ASM) technique. The dynamic coarse model is a combination of an evolutionary equivalent-circuit model and an efficient quasi-static numerical electromagnetic (EM) model—partial-element equivalent-circuit model. Namely, there are two forms of coarse models jointly in use: the coarse schematic model and the coarse EM model. The coarse schematic model evolutionarily incorporates parasitic effects that can be extracted from its accompanying coarse EM model. This process can greatly facilitate the original ASM process by easily determining a "high-quality" optimized coarse model. Two LTCC frequency-selective passive modules, i.e., a bandpass filter and a diplexer, are designed using the proposed scheme and ASM. No nonuniqueness in parameter extraction is encountered. Good convergence performance is achieved for the designs of both modules.**

***Index Terms*—Aggressive space mapping (ASM), diplexer, filter, low-temperature co-fired ceramic (LTCC), optimization, partial-element equivalent-circuit model (PEEC).**

I. Introduction

THE DEGREE OF integration of RF or microwave modules has mainly depended on the dimensions of the associated passive circuits. With the recent advances in low-temperature co-fired ceramic (LTCC) technology, more and more passive components and functional circuits have been buried in a ceramic substrate in a three-dimensional (3-D) fashion. As a result, the overall size of an RF sub-system can be significantly reduced. Generally, to satisfy prescribed specifications of an LTCC embedded circuit, an efficient optimization process is absolutely necessary. Traditional optimization schemes update design parameters either with the gradient information or an exhaustive search through intensive full-wave electromagnetic (EM) simulation. Usually, in practice, the expensive computation overhead prohibits LTCC circuits from being fully optimized.

Fortunately, an effective optimization scheme, called the aggressive space mapping (ASM) algorithm, was developed by Bandler *et al.* in 1995 [1]. The algorithm makes use of available experience (namely, coarse model) to reduce the workload of accurate EM simulation. However, the difficulty in the parameter extraction may sometimes cause the space-mapping algorithm to fail. To tackle this problem, several mathematical efforts are taken to improve the parameter-extraction process in the original ASM algorithm [2]–[5]. All of the improvements will undoubtedly increase the complexity and computational overhead. As a matter of fact, the difficulties arising in parameter extraction are mainly due to the lack of physical essence for the coarse model. It is found that, for LTCC circuit design particularly, if we add sufficient physical knowledge in the coarse model by including parasitic effects, e.g., the ASM algorithm, can still converge fast.

In this paper, an efficient static EM model, namely, the partial-element equivalent-circuit (PEEC) algorithm, will partially serve as the coarse model in ASM. In order to obtain the optimal coarse model solution, a schematic circuit model will also be employed together with the PEEC model. The proposed optimization procedure begins with an ideal schematic model. A curve-fitting process is performed with the PEEC model to obtain the physical dimensions and a better quality updated schematic model that takes parasitic effects into account. The updated schematic circuit model is then further optimized. This leads to a set of updated physical dimensions by performing a curve-fitting process based on the response of the updated schematic model.

To demonstrate the effectiveness of the proposed dynamic coarse model, a lumped-element bandpass filter with two finite transmission zeros and a lumped element diplexer for dual band [global system for mobile communications (GSM)/digital communications system (DCS)] mobile handset are designed with good convergence performance.

II. Basic Concepts

A. Basic Concepts of ASM

The ASM technique has been proven to be an efficient approach for microwave circuit optimization design [1]–[7]. In the technique, two models are involved. One is an accurate, but time-consuming model, called the fine model. The other one is a less accurate, but much more efficient model, denoted as the coarse model. ASM establishes a mathematical link (mapping) between the spaces of the parameters of the two models. It exploits Broyden's formula to quantitatively predict the new dimension parameters through the parameter extraction for mapping the fine model responses to those of the coarse model. In such a way, most of simulations are carried out with the coarse

Manuscript received January 4, 2003; revised May 28, 2003.

K.-L. Wu, J. Wang, and M. K. K. Cheng are with the Department of Electronic Engineering, Chinese University of Hong Kong, Shatin, Hong Kong.

Y.-J. Zhao is with the School of Mechano-Electronic Engineering, Xidian University, Xi'an 710071, China.

Digital Object Identifier 10.1109/TMTT.2003.820901

model and only one fine model simulation is needed in each ASM iteration.

B. Fundamentals of PEEC

The PEEC algorithm was originally developed by Ruehli [8] for modeling 3-D multiconductor systems. The basic idea of the PEEC is to convert the original structure to a network of discrete resistors, inductors, and capacitors (called the partial elements) by properly discretizing the mixed-potential integral equation. The partial elements of capacitors and inductors are first calculated by closed formula and the resultant equivalent circuit can then be solved with a conventional circuit theory.

For a system of K conductors, the mixed-potential integral equation can lead to

$$E_x^i(\mathbf{r},t) = \frac{J_x(\mathbf{r},t)}{\sigma} + \sum_{k=1}^{K}\sum_{n}\frac{\mu}{4\pi}\left[\int_{v_n} G(\mathbf{r},\mathbf{r}')dv_n'\right]\frac{\partial J_n^x(t')}{\partial t} + \sum_{k=1}^{K}\sum_{m}\frac{1}{4\pi\varepsilon}\frac{\partial}{\partial x}\left[q_m(t')\int_{s_m} G(\mathbf{r},\mathbf{r}')ds_m'\right] \quad (1)$$

where $G(\mathbf{r},\mathbf{r}')$ is the associated Green's function and current $\boldsymbol{J}$ and q are expended with pulse functions.

For conciseness, only the x-component of the equation is presented. By applying the Galerkin matching procedure to the above equation and set incident field to zero, we can have

$$0 = V_R + V_L + V_C \quad (2)$$

where the terms on the right-hand side represent the resistive, inductive, and capacitive voltage drops across the matched volume cell, respectively.

For perfect conductors, the first term should be zero. The second term can be rewritten in terms of total current through the nth volume cell as

$$V_L = \sum_{k=1}^{K}\sum_{n}\left\{\frac{\mu}{4\pi}\frac{1}{a_l a_n}\left[\int_{v_l}\int_{v_n} G(\mathbf{r},\mathbf{r}')dv_n' dv_l\right]\right\}\frac{\partial I_n^x(t')}{\partial t} = \sum_{k=1}^{K}\sum_{n} Lp_{l,n}\frac{dI_n^x(t')}{dt}. \quad (3)$$

This equation clearly suggests itself as a voltage–current relationship of an inductor with mutual coupling from other inductors.

The third term can be finally expressed as

$$V_C = \sum_{k=1}^{K}\sum_{m}\frac{q_m(t')}{4\pi\varepsilon} \times \left[\int_{s_m} G\left(\mathbf{r}_l^+,\mathbf{r}'\right)ds_m' - \int_{s_m} G\left(\mathbf{r}_l^-,\mathbf{r}'\right)ds_m'\right] \quad (4)$$

or in terms of total charge over the mth surface cell

$$V_C = \sum_{k=1}^{K}\sum_{m}\left\{\frac{1}{4\pi\varepsilon}\frac{1}{S_m}\left[\int_{s_m} G\left(\mathbf{r}_l^+,\mathbf{r}'\right)ds_m' - \int_{s_m} G\left(\mathbf{r}_l^-,\mathbf{r}'\right)ds_m'\right]\right\}Q_m(t') \quad (5)$$

where $\mathbf{r}_l^+ = (x_l+\Delta x_l/2, y_l, z_l)$ and $\mathbf{r}_l^- = (x_l-\Delta x_l/2, y_l, z_l)$.

Clearly, again, the inverse of the matrix composed of terms in the curly bracket coincide with the partial capacitance matrix.

Since the size of the LTCC circuit is, in general, much smaller than the operating wavelength, and that the accuracy of the PEEC coarse model is not as critical as its speed, a quasi-static approximation is made. Therefore, the retardation time can be neglected and the Green's function can take the form of static one. Once the partial elements are calculated, the response can be solved with well-developed circuit theory. It is worth mentioning that, by removing some unessential nodes, the simplified partial network model can be analyzed much faster than the full-wave EM solvers.

C. Concept of Dynamic Coarse Model

A high-quality coarse model is essential in applying ASM. We adopt the PEEC model as the coarse model since it has been proven very fast with acceptable accuracy, especially in the lower frequency range, in which most of the LTCC modules work. To determine the optimal coarse model, a schematic equivalent-circuit model is first employed, which acts as a part of the coarse model. The equivalent-circuit model and PEEC model are associated with each other and work in a coordinated fashion to obtain the optimal coarse model. For convenience, we call the two models the coarse schematic model $\mathbf{x}_{cs}^{(i)}$ and coarse EM model $\mathbf{x}_{\text{cem}}^{(i)}$, respectively.

The proposed dynamic coarse model begins with an ideal schematic circuit. Although it can hardly fully characterize an LTCC circuit before all parasitic effects are taken into account, the ideal schematic circuit provides a straightforward guidance as far as the initial design is concerned. The detail procedure for obtaining the optimal coarse model using the dynamic coarse model concept is illustrated in the flowchart shown in Fig. 1.

First of all, an ideal (without parasitic elements) coarse schematic model is created by intuition and is optimized to satisfy the desired specifications. The optimal component values are denoted as

$$\mathbf{x}_{cs}^* = \underset{\mathbf{x}_{cs}}{\text{Opt}}\left(R_{cs}(\mathbf{x}_{cs})\right). \quad (6)$$

The initial dimensions $\mathbf{x}_{\text{cem}}^{(i)}$ of each inductor or capacitor can then be roughly estimated by either the fitting response of a single component or by using empirical formulas [7]. Having had all the component dimensions determined, the whole circuit geometry can be constructed.

By curve fitting the coarse EM model response as close as possible to that of the optimal ideal coarse schematic model and

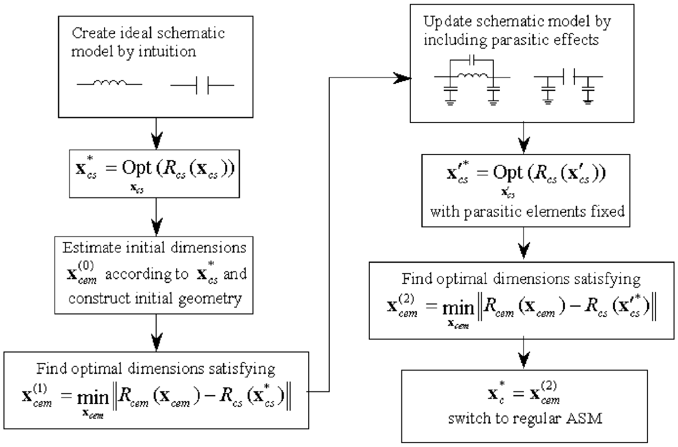

Fig. 1. Flowchart for obtaining optimal coarse model.

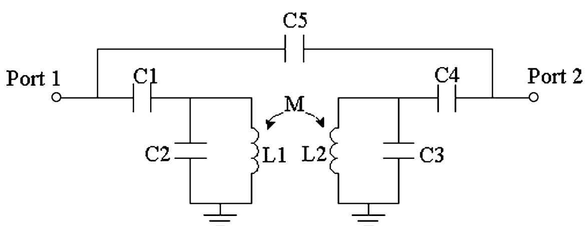

Fig. 2. Schematics of the bandpass filter.

TABLE I
PARAMETERS IN COARSE SCHEMATIC MODEL AND COARSE EM MODEL OF THE BANDPASS FILTER

$\mathbf{x}_{cs}^*$		$\mathbf{x}_{cem}^{(1)}$ (mils)		$\mathbf{x}_{cs}'^*$		$\mathbf{x}_c^* = \mathbf{x}_{cem}^{(2)}$ (mils)	
$C1$	0.705 pF	$W1$	45	$C1$	0.624 pF	$W1$	45
$C2$	2.373 pF	$W2$	30	$C2$	1.731 pF	$W2$	30
$C3$	2.373 pF	$W3$	15	$C3$	1.731 pF	$W3$	15
$C4$	0.705 pF	$H1$	62.65	$C4$	0.624 pF	$H1$	62.37
$C5$	0.068 pF	$H2$	30.10	$C5$	0.059 pF	$H2$	30.19
$L1$	1.396 nH	$H3$	14.04	$L1$	1.782 nH	$H3$	13.17
$L2$	1.396 nH	$L1$	70.63	$L2$	1.782 nH	$L1$	71.06
M	0.164 nH	$L2$	40.46	M	0.257 nH	$L2$	41.45

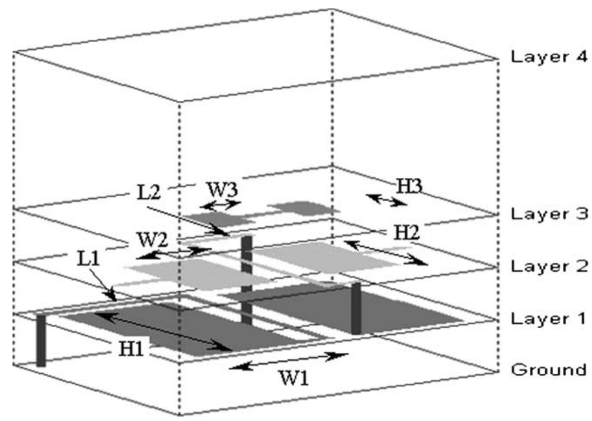

Fig. 3. LTCC layout of the multilayer bandpass filter.

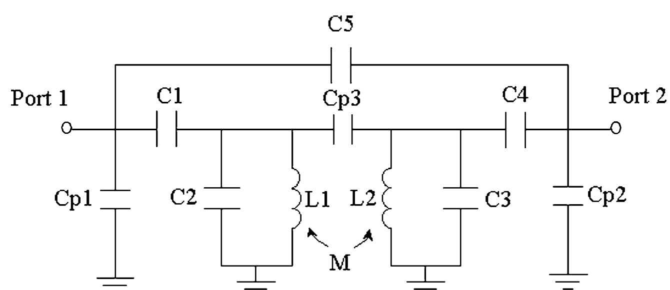

Fig. 4. Coarse schematic model with parasitic elements.

systematically recombining and removing some of unessential nodes in the resultant PEEC network model, the new coarse schematic model with parasitic components can be obtained. Generally, the response of this updated schematic model may differ from that of the ideal one. We need to optimize the coarse schematic model again to meet the specifications. It is worth mentioning that, unlike the parasitic component for a cascaded coarse model in [9], which is extracted by intuition and curving fitting, the physically expressive parasitic network in our updated schematic model is systematically derived. The detail of the derivation process will be discussed in a future publication.

It is known that when physical dimensions change insignificantly, parasitic effects will not change as rapid as those of the main components. Keeping this in mind, we now optimize the updated coarse schematic model with parasitic components fixed; that is to say, only main components are adjusted. New component values in the coarse schematic model are obtained as

$$\mathbf{x}_{cs}'^* = \underset{\mathbf{x}_{cs}'}{\mathrm{Opt}}\left(R_{cs}(\mathbf{x}_{cs}')\right). \tag{7}$$

To get the geometric dimensions corresponding to $\mathbf{x}_{cs}'^*$, another curve-fitting procedure is applied. Up to this stage, much better agreement between the coarse EM model response and coarse schematic model can be achieved because parasitic effects are considered in both models. Repeat the above process until the specifications are satisfied by the coarse EM model.

After an optimal coarse EM model is obtained, it is assigned as the coarse model in the standard ASM procedure in which the optimal solution of the coarse EM model is denoted as $\mathbf{x}_c^*$.

It can be noted that the word "dynamic" has two meanings here. One is that the coarse schematic model evolves from the one without parasitic effects to the one with parasitic effects in the stage of obtaining $\mathbf{x}_c^*$; the other is that the coarse model switches from the combination of the equivalent-circuit model and PEEC model to a pure PEEC model once $\mathbf{x}_c^*$ is available.

One may be concerned with why we do not optimize the dimensions in the coarse EM model directly after the whole geometry is constructed instead of optimizing the coarse schematic model first and getting the optimal dimensions by curve fitting. This is because there may exist more than one local minimum in the coarse EM model. We found that this optimal solution by curve fitting the circuit model response can be obtained with better certainty.

III. Design Examples

Two LTCC frequency-selective passive modules are designed by the proposed dynamic coarse model with the ASM proce-

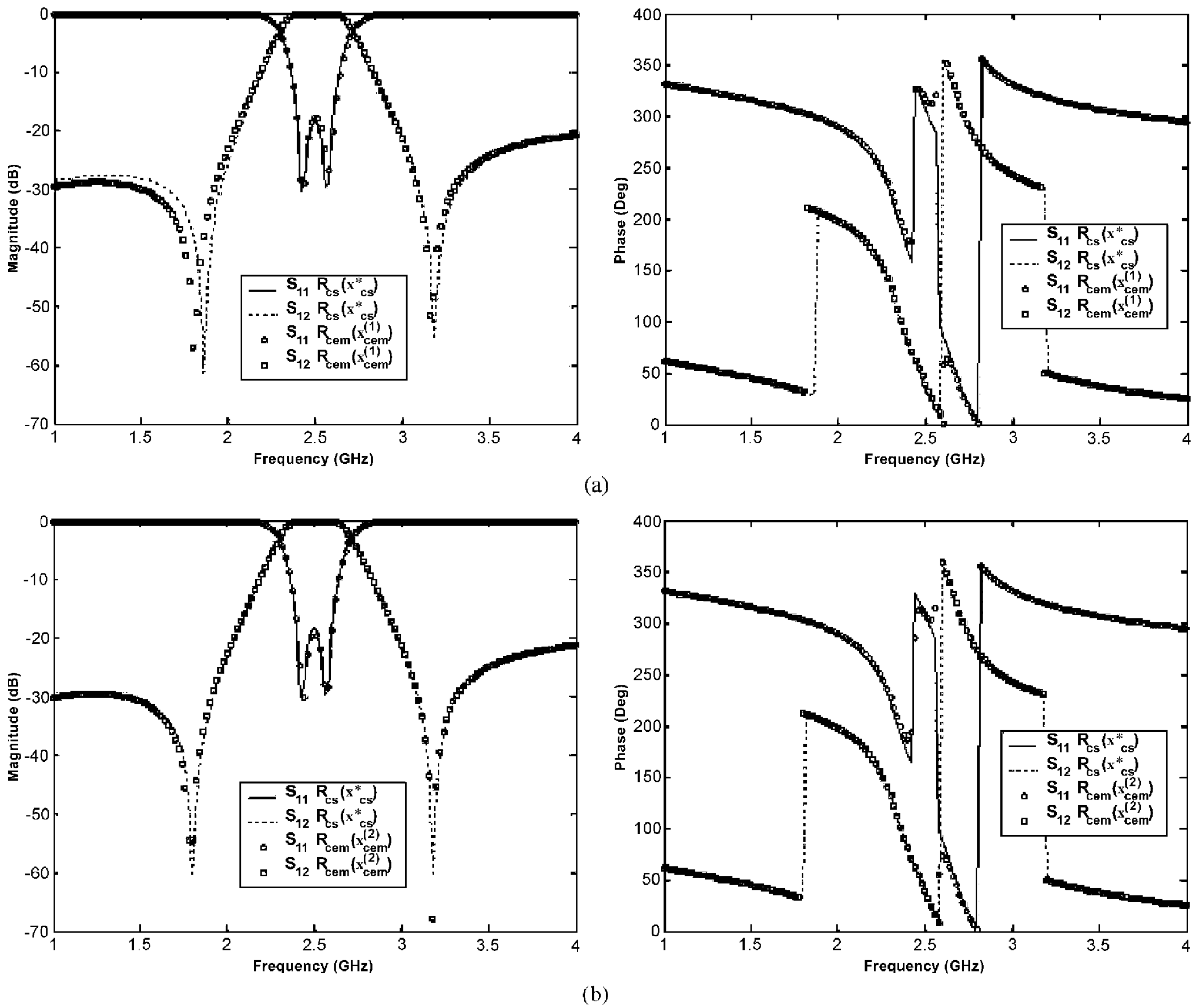

Fig. 5. Extraction of coarse EM model from the coarse schematic model.

dure. One is a compact bandpass filter with two finite transmission zeros [10]. The other is a multilayer dual band diplexer for a (GSM/DCS) mobile phone.

A. Compact Bandpass Filter

Fig. 2 shows the ideal schematic circuit of a compact bandpass filter. The optimal component values are determined according to specifications and are listed in the second column of Table I. The corresponding LTCC layout with the design parameters indicated is shown in Fig. 3. The thickness of substrate layers is 3.6 mil for layers 1–3 and 10.8 mil for layer 4. The dielectric constant is 7.8.

The optimal dimensions $\mathbf{x}_{\rm cem}^{(1)}$ at which the coarse EM model response fits that of the optimal schematic circuit model $\mathbf{x}_{cs}^{*}$ are extracted and are given in column 2 of Table I. $W1$–$W3$ are kept constant in the optimization. At the same time, an updated schematic model in which parasitic effects are taken into account is obtained and drawn in Fig. 4. By optimizing the updated circuit model with parasitic components $Cp1 = 0.075$ pF, $Cp2 = 0.069$ pF, and $Cp3 = 0.062$ pF as constants, the new main component values $\mathbf{x}_{cs}^{\prime *}$ are obtained and are listed in column 3 of Table I. By taking another parameter extrac-

TABLE II
FINE MODEL PARAMETERS AND EXTRACTED COARSE MODEL PARAMETERS OF THE BANDPASS FILTER

Step	$j = 1$	$j = 2$	$j = 3$	$j = 4$
	45	45	45	45
	30	30	30	30
	15	15	15	15
	62.36470	65.59380	65.90371	65.64838
$\mathbf{x}_f^{(j)}$	30.19210	26.42520	27.61653	27.85812
	13.16840	8.23690	8.03906	7.69199
	71.06090	63.39920	61.02136	62.03204
	41.45270	29.82760	33.06622	33.63494
	45	45	45	
	30	30	30	
	15	15	15	Unit: mils
	59.13560	62.02400	62.60360	
$\mathbf{x}_c^{(j)}$	33.95900	28.88240	29.86880	
	18.09990	13.38590	13.53410	$\mathbf{x}_f^{(1)} = \mathbf{x}_c^{*}$
	78.72260	73.67500	70.19600	
	53.07780	37.89230	40.65370	

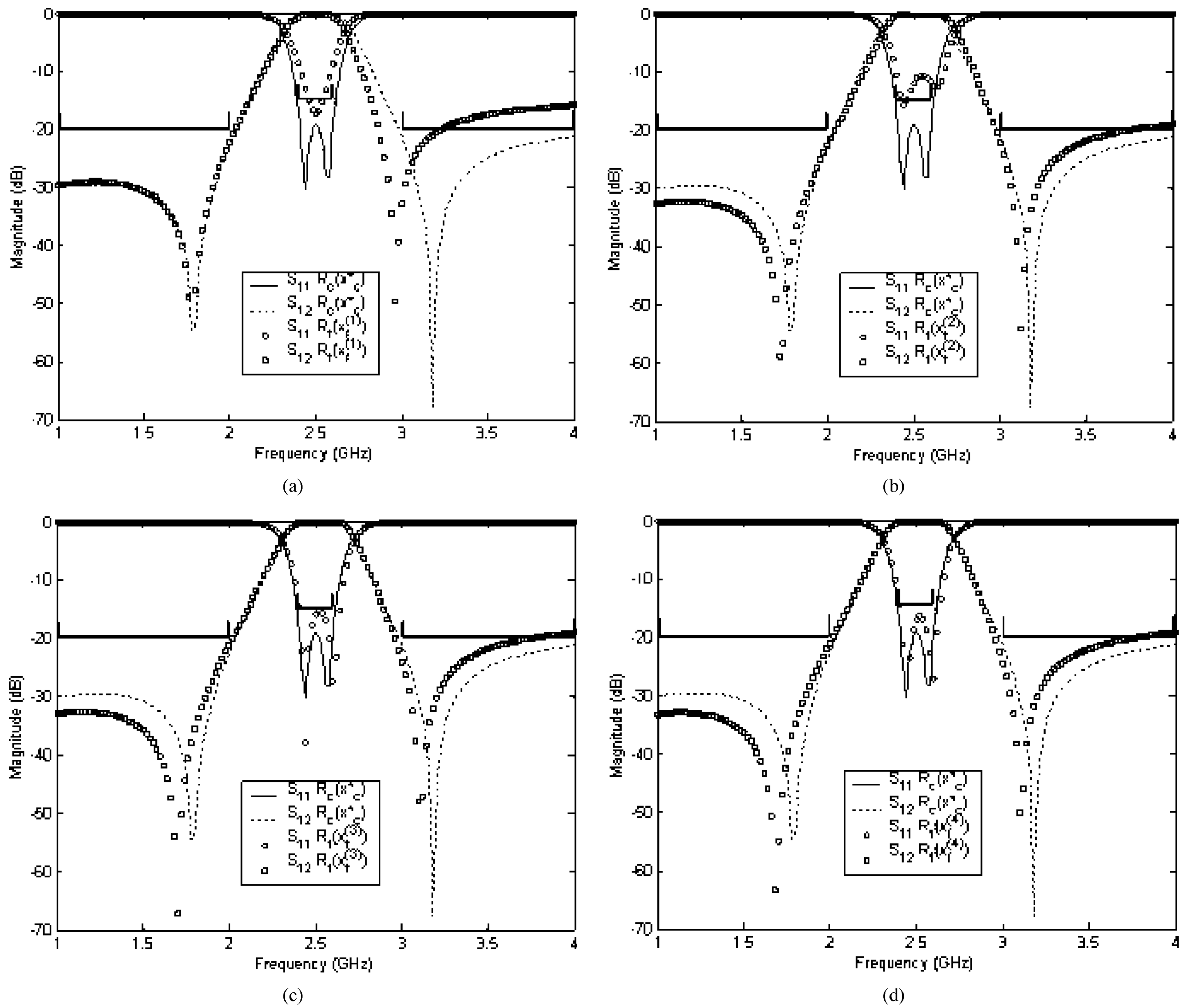

Fig. 6. Fine model response of the bandpass filter at $\mathbf{x}_f^{(j)}$. (a) $j = 1$ (starting point). (b) $j = 2$. (c) $j = 3$, (d) $j = 4$.

tion, the final optimal dimensions $\mathbf{x}_{\text{cem}}^{(2)}$ in the coarse EM model can be obtained by fitting the PEEC model response to that of the updated schematic model as close as possible. Once the responses of the coarse EM model $R(\mathbf{x}_{\text{cem}}^{(*)})$ satisfies the required specifications, the optimal coarse model solution is set to be $\mathbf{x}_c^* = \mathbf{x}_{\text{cem}}^{(*)}$, which is shown in the last column of Table I.

To illustrate the effectiveness of the proposed dynamic coarse model, the comparison of the responses of the coarse EM model with those of the coarse schematic model is shown in Fig. 5.

Once the optimal coarse model is determined, the optimization procedure continues with regular ASM and the coarse model turns to be a pure PEEC model. The fine model used for this example is IE3D, a full-wave EM simulator of Zeland Software, Fremont, CA. It is worth mentioning that the computing time of a single frequency sweep for the PEEC model and IE3D model are approximately 2 and 94 s, respectively. After only three updates of the fine model parameters, the extracted coarse model comes very close to $\mathbf{x}_c^*$ and the fine model response becomes converged. To provide a clear picture of the convergence, the design parameters in both models are listed in Table II.

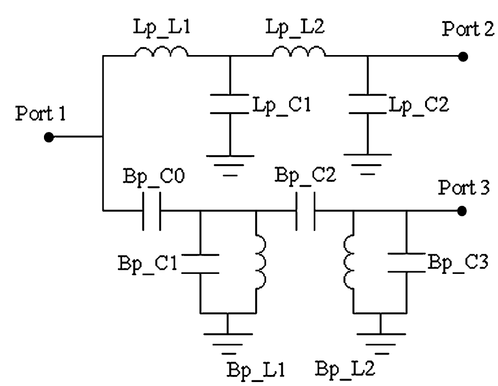

Fig. 7. Ideal schematic model of the diplexer.

The progressive improvement of the fine model response from the starting point to the end point that satisfies the specifications is given in Fig. 6. As a reference, the optimal coarse model response is also superposed.

TABLE III
PARAMETERS IN COARSE SCHEMATIC MODEL AND COARSE EM MODEL OF THE DIPLEXER

$\mathbf{x}_{cs}^{*}$		$\mathbf{x}_{cem}^{(1)}$ (mils)		$\mathbf{x}_{cs}^{\prime *}$		$\mathbf{x}_{c}^{*} = \mathbf{x}_{cem}^{(2)}$ (mils)	
Lp_L1	10.377 nH	Ly_Lp_L1	37.445	Lp_L1	10.506 nH	Ly_Lp_L1	36.962
Lp_L2	10.567 nH	Ly_Lp_L2	61.556	Lp_L2	10.312 nH	Ly_Lp_L2	61.482
Lp_C1	6.893 pF	Wy_Lp_C1	46.212	Lp_C1	4.489 pF	Wy_Lp_C1	45.853
Lp_C2	3.784 pF	Wy_Lp_C2	36.083	Lp_C2	3.512 pF	Wy_Lp_C2	36.167
Bp_C0	3.607 pF	Wy_Bp_C0	31.039	Bp_C0	2.300 pF	Wy_Bp_C0	30.112
Bp_C1	7.811 pF	Wy_Bp_C1	21.611	Bp_C1	0.787 pF	Wy_Bp_C1	21.245
Bp_C2	2.327 pF	Wy_Bp_C2	21.966	Bp_C2	1.455 pF	Wy_Bp_C2	22.163
Bp_C3	6.089 pF	Wy_Bp_C3	28.552	Bp_C3	4.103 pF	Wy_Bp_C3	29.010
Bp_L1	0.776 nH	Ly_Bp_L1	33.879	Bp_L1	1.667 nH	Ly_Bp_L1	34.052
Bp_L2	0.962 nH	Ly_Bp_L2	20.516	Bp_L2	1.042 nH	Ly_Bp_L2	20.433

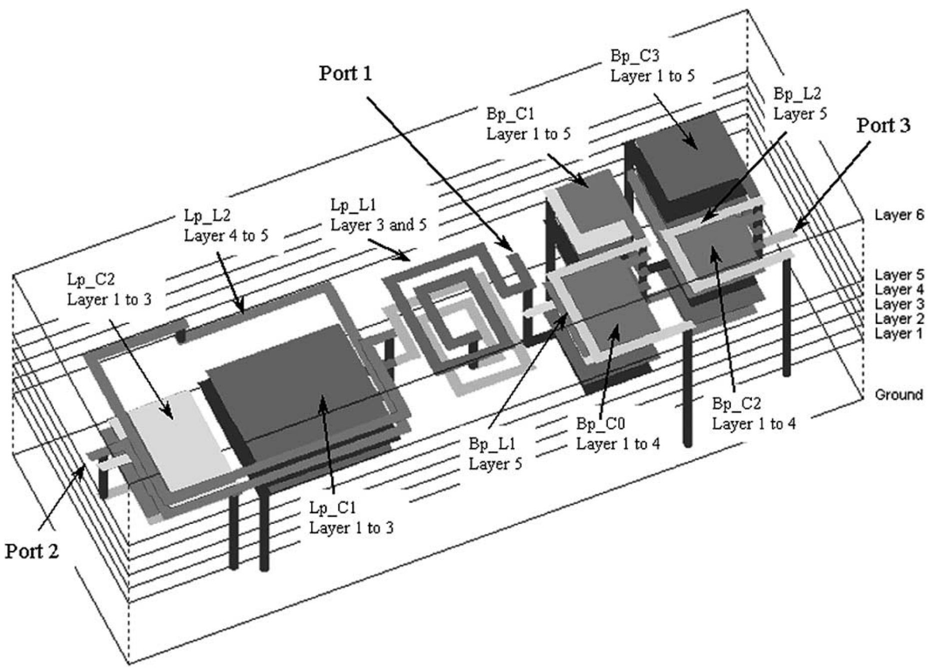

Fig. 8. Layout of the LTCC diplexer.

B. *Diplexer for Dual-Band (GSM/DCS) Mobile Phone*

The ideal schematic circuit of a diplexer is shown in Fig. 7. The diplexer is composed of a low-pass filter and bandpass filter. The specifications of the diplexer are $|S_{11}| < -16$ dB, $|S_{12}| > -0.8$ dB, and $|S_{13}| < -30$ dB, and the frequency band of 880–960 MHz and $|S_{11}| < -16$ dB, $|S_{12}| < -30$ dB, and $|S_{13}| > -1.0$ dB are in the 1710–1990-MHz band. The optimal component values at which the specifications are satisfied are shown in the first column of Table III.

According to the component values, the initial LTCC layout is constructed and is shown in Fig. 8. The thickness of layer 1 and layer 6 is 3.5433 mil and that of layers 2–5 is 1.6929 mil. The relative dielectric constant is 7.8.

The optimal coarse model dimensions $\mathbf{x}_{\rm cem}^{(1)}$ can be extracted by fitting the responses of the PEEC model with those of the ideal optimal schematic model whose component values are listed in the first column of Table III. Dimensions of capacitors and inductors along the x-direction (along the longer side) are fixed at $Lx\_LP\_L1 = 30$, $Lx\_LP = \_L2 = 85$, $Wx\_LP\_C1 = 50$, $Wx\_LP\_C2 = 30$, $Wx\_BP\_C0 = 25$, $Wx\_BP\_C1 = 20$, $Wx\_BP\_C2 = 25$, $Wx\_BP\_C3 = 30$, $Lx\_BP\_L1 = 30$, and $Lx\_BP\_L2 = 30$, where the unit is mils. Dimensions along the y-direction are adjusted and the optimal result is listed in column 2 of Table III. From a previous PEEC analysis, the updated coarse schematic model in which parasitic effects are considered can be obtained, as shown in Fig. 9. Keeping the values of the parasitic components fixed, we can further adjust the main component values $\mathbf{x}_{cs}^{\prime *}$ to satisfy the required specifications by optimization. The updated values of the main components are shown in column 3 of Table III. The values of parasitic components are $Lp\_Cp1 = 0.404$ pF, $Lp\_Cp2 = 1.917$ pF, $Lp\_Cp3 = 0.093$ pF, $Lp\_Cp4 = 0.244$ pF, $Lp\_Lp1 = 0.398$ nH, $Bp\_Cp1 = 0.404$ pF, $Bp\_Cp2 = 0.203$ pF, $Bp\_Cp3 = 0.20$ pF, $Bp\_Cp4 = 1.477$ pF, $Bp\_Cp5 = 1.225$ pF, $Bp\_Lp1 = 0.541$ nH, and $Bp\_Lp2 = 0.307$ nH.

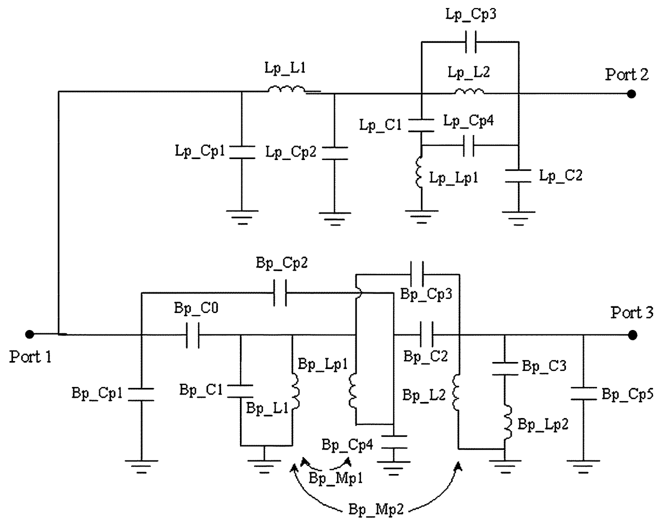

Fig. 9. Updated coarse schematic model with parasitic effects.

TABLE IV
FINE MODEL PARAMETERS AND EXTRACTED COARSE MODEL PARAMETERS OF THE DIPLEXER DESIGN

Step	$j = 1$	$j = 2$	$j = 3$	$j = 4$
$\mathbf{x}_f^{(j)}$	36.9624	45.7417	47.2332	46.5078
	61.4822	68.2006	76.2548	75.6720
	45.8534	44.1208	38.5771	38.7108
	36.1669	36.9349	32.3949	32.8295
	30.1122	27.4853	24.7291	25.4450
	21.2459	17.1060	12.1577	13.3557
	22.1636	22.2326	15.9666	19.5793
	29.0104	24.1138	24.205	24.7073
	34.0521	46.9804	59.6386	63.5015
	20.4335	34.6538	36.0031	38.8587
$\mathbf{x}_c^{(j)}$	28.1831	35.9818	37.7866	
	54.7638	56.1869	62.7793	
	47.5860	49.4981	45.2107	
	35.3989	39.1517	35.3299	Unit: mils
	32.7391	31.9243	29.1661	
	25.3858	24.4992	19.6154	$\mathbf{x}_f^{(1)} = \mathbf{x}_c^*$
	22.0946	26.2832	18.0827	
	33.9070	28.9504	28.5359	
	21.1238	25.7299	31.7528	
	6.21320	19.5464	17.8366	

Having had the more realistic optimized coarse schematic model by taking the parasitic effects into account, the optimized coarse EM model can then be extracted and is considered as the optimal coarse model $\mathbf{x}_c^*$ in the ASM procedure.

The fine model for the diplexer design is HFSS, a full-wave EM finite-element method solver of the Ansoft Corporation, Pittsburgh, PA. However, the difference between the speed of the coarse EM model and the fine EM model (HFSS) for this example is remarkable. The computation time of a single frequency sweep is 166 s with the PEEC model and is 3677 s with HFSS.

Three iterations of the fine model updates are need in ASM to take the fine model response close enough to the optimal coarse model response. The parameters at each iteration are summarized in Table IV.

The comparison of S-parameters of the coarse EM model and the fine model for parameters extraction at each ASM iteration is shown in Fig. 10(a)–(c). Since the coarse EM model can reflect all the static capacitive and inductive couplings, it can be observed from Fig. 10(a)–(c) that the coarse model responses $R_c(\mathbf{x}_c^{(i)})$ can catch all the detailed variations of the fine model responses $R_f(\mathbf{x}_f^{(i)})$ very well.

The convergence of the fine model responses is demonstrated in Fig. 11.

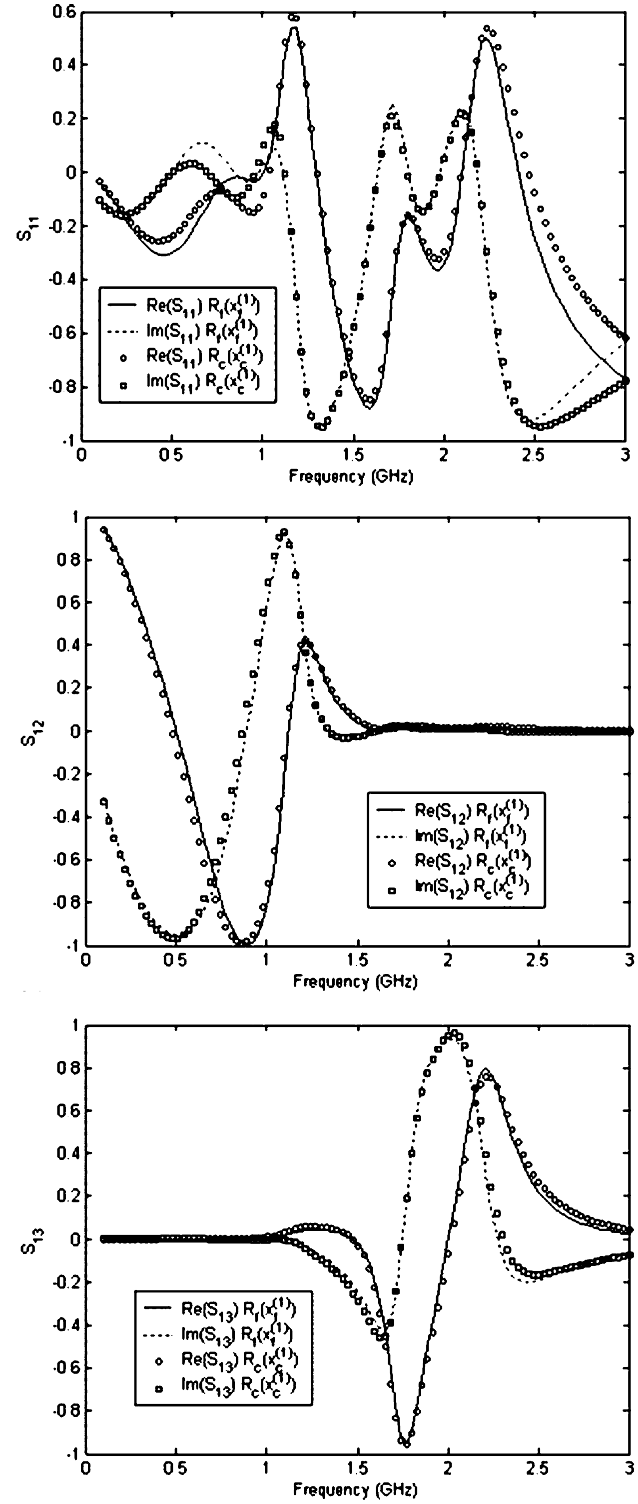

(a)

Fig. 10. Comparison of S-parameters of the coarse model response and the fine model response in each parameters extraction of the diplexer design. (a) $j = 1$.

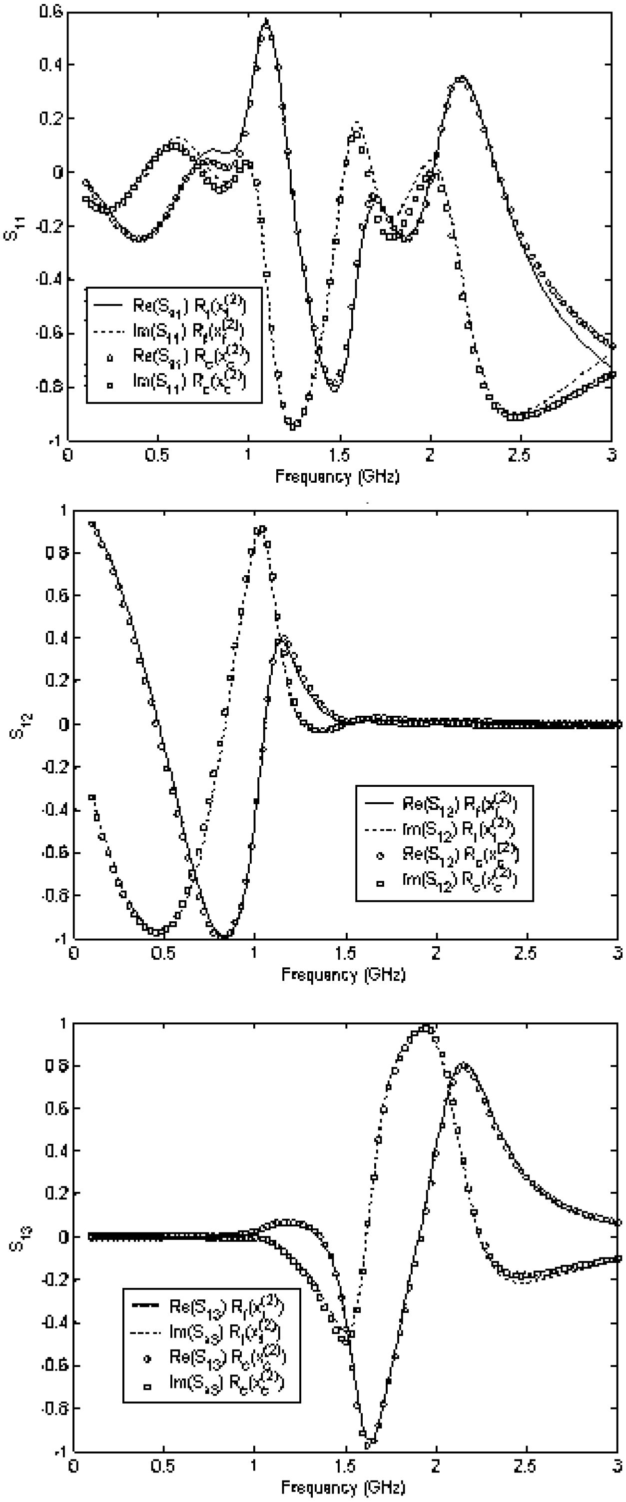

(b)

Fig. 10. *(Continued.)* Comparison of S-parameters of the coarse model response and the fine model response in each parameters extraction of the diplexer design. (b) $j = 2$.

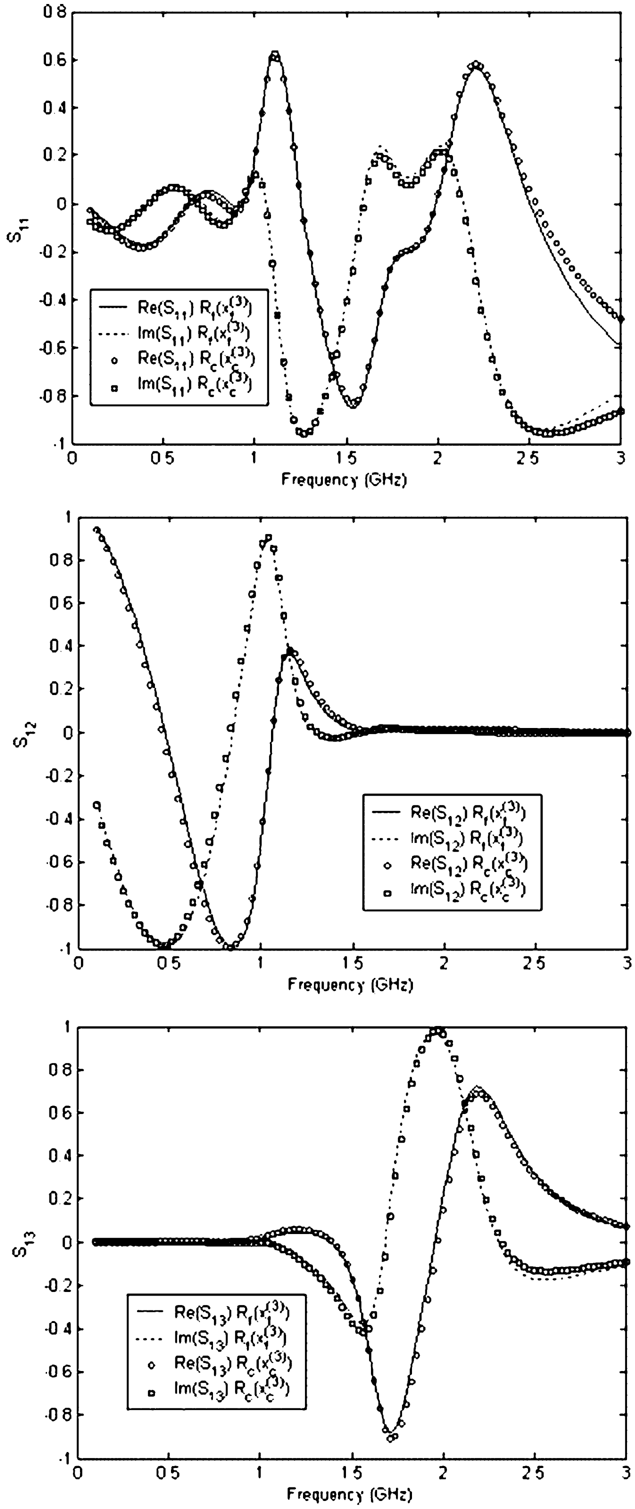

(c)

Fig. 10. *(Continued.)* Comparison of S-parameters of the coarse model response and the fine model response in each parameters extraction of the diplexer design. (c) $j = 3$.

IV. Conclusion

In this paper, a new concept of a dynamic coarse model for an ASM algorithm is proposed and is applied to the optimization design of LTCC RF circuits. It is initially a combination of an evolutionary equivalent-circuit model and an efficient quasi-static PEEC model in determining the optimal coarse model solution. The coarse model is then switched to the pure PEEC model in the traditional space-mapping process. The dynamic coarse model can easily incorporate the parasitic effects so that it facilitates the process of finding a

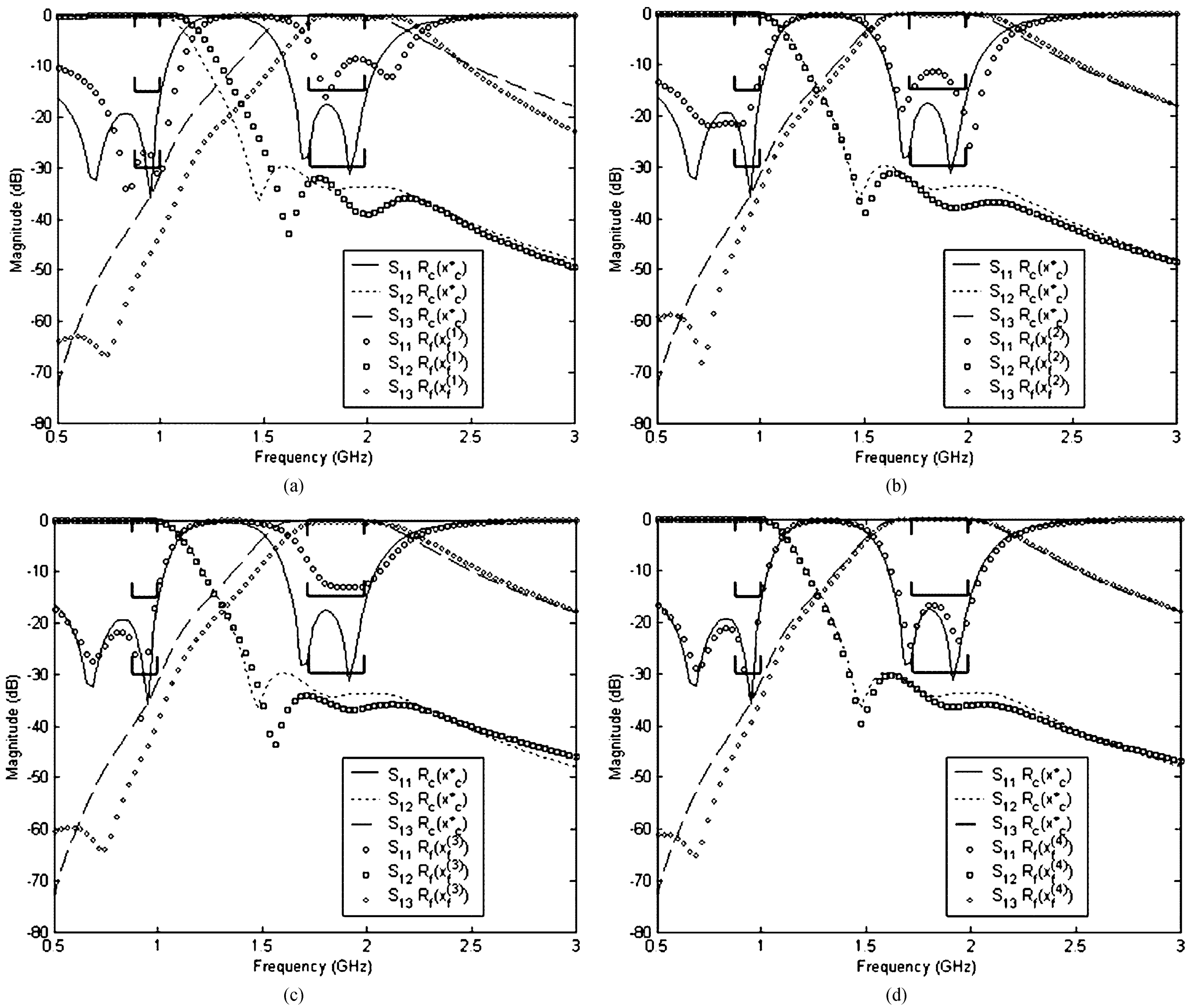

Fig. 11. Convergence of the fine model responses of the diplexer design at $\mathbf{x}_f^{(j)}$. (a) $j = 1$(starting point). (b) $j = 2$. (c) $j = 3$. (d) $j = 4$ (ending point).

"high-quality" optimized coarse model for ASM. A bandpass filter and a diplexer in a dual-band mobile phone are designed using this dynamic coarse model with full-wave commercial EM simulation software IE3D and HFSS adopted as the fine model, respectively. Good convergence performance is achieved in both module designs in only three steps of fine model parameter update and, consequently, only three fine model simulations are needed. Since the dynamic coarse model that can properly characterize the parasitic effects in an LTCC circuit is utilized, no problem of nonuniqueness is encountered in parameter extraction.

REFERENCES

[1] J. W. Bandler, R. M. Bierncki, S. H. Chen, R. H. Hemmers, and K. Madsen, "Electromagnetic optimization exploiting aggressive space mapping," *IEEE Trans. Microwave Theory Tech.*, vol. 43, pp. 2874–2881, Dec. 1995.

[2] M. H. Bakr and J. W. Bandler, "Review of the space mapping approach to engineering optimization and modeling," *Opt. Eng.*, no. 1, pp. 241–276, 2000.

[3] J. W. Bandler, R. M. Biernacki, and S. H. Chen, "Fully automated space mapping optimization of 3D structures," in *IEEE MTT-S Int. Microwave Symp. Dig.*, 1996, pp. 753–756.

[4] M. H. Bakr, J. W. Bandler, R. M. Biernacki, S. H. Chen, and K. Madsen, "A trust region aggressive space mapping algorithm for EM optimization," *IEEE Trans. Microwave Theory Tech.*, vol. 46, pp. 2412–2425, Dec. 1998.

[5] M. H. Bakr, J. W. Bandler, and N. Georgieva, "An aggressive approach to parameter extraction," *IEEE Trans. Microwave Theory Tech.*, vol. 47, pp. 2428–2439, Dec. 1999.

[6] M. H. Bakr, J. W. Bandler, J. E. Rayas-Sanchez, and J. Sondergaard, "Space-mapping optimization of microwave circuits exploiting surrogate models," *IEEE Trans. Microwave Theory Tech.*, vol. 48, pp. 2297–2306, Dec. 2000.

[7] K.-L. Wu, R. Zhang, M. Ehlert, and D.-G. Fang, "An explicit knowledge-embedded space mapping technique and its application to optimization of LTCC RF passive circuits," *IEEE Trans. Comp. Packag. Technol.*, vol. 26, pp. 399–406, June 2003.

[8] A. E. Ruehli, "Equivalent circuit models for three-dimensional multi-conductor systems," *IEEE Trans. Microwave Theory Tech.*, vol. MTT-22, pp. 216–221, Mar. 1974.

[9] S. Ye and R. R. Mansour, "An innovative CAD technique for microstrip filter design," *IEEE Trans. Microwave Theory Tech.*, vol. 45, pp. 780–786, May 1997.

[10] L. K. Yeung and K.-L. Wu, "A compact second-order LTCC band-pass filter with two finite transmission zeros," *IEEE Trans. Microwave Theory Tech.*, vol. 51, pp. 337–341, Feb. 2003.

Ke-Li Wu (M'90–SM'96) received the B.S. and M.Eng. degrees from the Nanjing University of Science and Technology, Nanjing, China, in 1982 and 1985, respectively, and the Ph.D. degree from Laval University, Quebec, QC, Canada, in 1989.

From 1989 to 1993, he was with the Communications Research Laboratory, McMaster University, Montreal, QC, Canada. In March 1993, he joined the Corporate Research and Development Division, Com Dev International, where he had been a Principal Member of Technical Staff in charge of developing advanced EM design software for various microwave subsystems. Since October 1999, he has been with the Department of Electronic Engineering, The Chinese University of Hong Kong, Shatin, Hong Kong, where he is a Professor. He has been published widely in the areas of EM modeling and microwave and antenna engineering. He holds one Canadian patent and one U.S. patent. His current research interests include all aspects related to LTCC multichip modules (MCMs) from EM modeling and design methodology to various applications.

Dr. Wu was a recipient of the 1992 URSI Young Scientist Award. He was also the recipient of the 1993 Industry Feedback Award presented by the Telecommunication Research Institute of Ontario and the 1998 Com Dev Achievement Award.

Yong-Jiu Zhao was born in Hebei Province, China, in 1964. He received the M.Eng. and Ph.D. degrees in electronic engineering from Xidian University, Xi'an, China, in 1990 and 1998, respectively.

Since March 1990, he has been with the Department of Measurement and Controlling Engineering and Instruments, School of Mechano-Electronic Engineering, Xidian University. From December 1999 to August 2000, he was a Research Associate with the Department of Electronic Engineering, The Chinese University of Hong Kong. His current fields of interest include computational electromagnetics and microwave components and subsystems.

Jie Wang was born in JiangSu Province, China, in 1975. He received the B.S. and Ph.D. degrees from the Southeast University of China, Nanjing, China, in 1996 and 2001, respectively, all in radio engineering. His doctoral dissertation concerned the investigation of the domain decomposition method (DDM) and parallel computation for full-wave analysis of two-dimensional (2-D) and 3-D scattering problems.

Since January 2002, he has been with the Chinese University of Hong Kong, Shatin, Hong Kong, where he is currently a Research Associate with the Department of Electronic Engineering. His current research interests include design and EM simulation of various LTCC embedded passives and integrated modules for wireless communications.

Michael K. K. Cheng (S'90–M'91) received the B.Sc. degree (with first-class honors) in electrical engineering and Ph.D. degree from King's College, University of London, London, U.K., in 1987 and 1993, respectively.

From 1990 to 1992, he was a Research Assistant with King's College, where he was involved in the area of hybrid circuit and monolithic microwave integrated circuit (MMIC) design. From 1993 to 1995, he was a Post-Doctoral Research Associate involved in the investigation of coplanar structures for microwave/millimeter-wave application. In 1996, he became an Assistant Professor with the Department of Electronic Engineering, The Chinese University of Hong Kong, Shatin, Hong Kong. He has authored or coauthored over 45 papers published in leading international journals and conferences, and was a contributing author of *MMIC Design* (London, U.K.: IEE Press, 1995) and *RFIC and MMIC Design and Technology* (London, U.K.: IEE Press, 2001). His current research interests are mainly concerned with the design of RF integrated circuits (RFICs)/MMICs, mixers, oscillators, power amplifiers, and linearization techniques.

Dr. Cheng was the recipient of the 1986 Siemens Prize, the 1987 Institution of Electrical Engineers Prize, and the 1988 Convocation Sesquicentennial Prize in Engineering (University of London).